sustainability

MDPI

Article

Forecasting of Carbon Emission in China Based on Gradient Boosting Decision Tree Optimized by Modified Whale Optimization Algorithm

Xiwen Cui [1,2,*], Shaojun E [3], Dongxiao Niu [1,2], Bosong Chen [1,2] and Jiaqi Feng [1]

[1] School of Economics and Management, North China Electric Power University, Beijing 102206, China; niudx@126.com (D.N.); cbs@ncepu.edu.cn (B.C.); fengjiaqi2019@hotmail.com (J.F.)
[2] Beijing Key Laboratory of New Energy and Low-Carbon Development, North China Electric Power University, Beijing 102206, China
[3] School of Information Science and Technology, Hebei Agricultural University, Baoding 071001, China; eshaojun@icloud.com
* Correspondence: 120202206100@ncepu.edu.cn

Abstract: As the global temperature continues to rise, people have become increasingly concerned about global climate change. In order to help China to effectively develop a carbon peak target completion plan, this paper proposes a carbon emission prediction model based on the improved whale algorithm-optimized gradient boosting decision tree, which combines four optimization methods and significantly improves the prediction accuracy. This paper uses historical data to verify the superiority of the gradient boosting tree prediction model optimized by the improved whale algorithm. In addition, this study also predicted the carbon emission values of China from 2020 to 2035 and compared them with the target values, concluding that China can accomplish the relevant target values, which suggests that this research has practical implications for China's future carbon emission reduction policies.

Keywords: gradient lifting tree; whale optimization algorithm; carbon emissions; carbon peak

check for updates

Citation: Cui, X.; E, S.; Niu, D.; Chen, B.; Feng, J. Forecasting of Carbon Emission in China Based on Gradient Boosting Decision Tree Optimized by Modified Whale Optimization Algorithm. *Sustainability* **2021**, *13*, 12302. https://doi.org/10.3390/su132112302

Academic Editor: Wen-Hsien Tsai

Received: 4 October 2021
Accepted: 1 November 2021
Published: 8 November 2021

Publisher's Note: MDPI stays neutral with regard to jurisdictional claims in published maps and institutional affiliations.

Copyright: © 2021 by the authors. Licensee MDPI, Basel, Switzerland. This article is an open access article distributed under the terms and conditions of the Creative Commons Attribution (CC BY) license (https://creativecommons.org/licenses/by/4.0/).

1. Introduction

As the world's largest developing country, China is also the world's largest carbon emitter [1]. Since entering the 21st century, China's carbon emissions have been growing rapidly, and its share in the world is also on the rise. In 2021, the terms carbon peak and carbon neutral were first written in the government's work report and became hot topics discussed by delegates. Xi Jinping, President of the People's Republic of China, stressed that the "14th Five-Year Plan" is a key period and a window period for a peak in carbon emissions, and an important plan needs to be made for the next five years to reduce carbon emissions, laying out a clear "construction plan" for the carbon emission peak in the 14th Five-Year Plan. In order to smoothly reduce carbon emissions, the accurate prediction of carbon emissions has become an important issue.

There are many kinds of prediction methods, such as the Bayes method [2–4], rule induction method [5,6] and KNN (K nearest neighbor) algorithm [7–10]. At present, the most widely used prediction methods are various algorithms in the field of artificial intelligence (AI), which are widely used because of their high computing speed and high computing precision.

Decision tree representation is one of the most widely used logic methods. It deduces the classification rules of decision tree representation from a group of unordered and irregular cases. Tso et al. used decision trees to predict electrical energy consumption [11]; Peng et al. used gradient driven regression trees to predict household energy consumption [12]. Decision tree analysis has been used to determine the influence factors of residents' carbon dioxide emissions under different travel modes [13]. One of the greatest advantages of the

decision tree-based classification algorithm is that it does not require the user to possess a large amount of background knowledge in the learning process; as long as the training examples can be represented by attribute conclusion, the algorithm can be used to learn [14]. The gradient boosting decision tree algorithm (GBDT) used in this paper is one of them.

Gradient boosting, first proposed by Friedman in 2001, is a supervised learning algorithm. When the GBDT algorithm and gradient boosting principle were proposed by Friedman, researchers were interested in their strong prediction performance [15]. Compared with other prediction methods, GBDT has high prediction accuracy and low consumption. It has been found that the stochastic gradient enhanced tree (GBDT) meets or exceeds the predictive performance of the SVM and the RF, is the fastest algorithm in predictive efficiency [16] and has much lower computational costs than those of other algorithms [17]. Moreover, under the same input combination, the GBDT model is superior to the M5Tree model and empirical model in prediction accuracy [18].

GBDT is being used for a variety of energy planning tasks. Fan and Lu used GBDT to predict regional water evapotranspiration (ET0) [17] and pan evaporation (EP) [18]; David et al. used GBDT to predict solar irradiance [19]; Amar et al. used GBDT to predict interfacial tension (IFT) in the crude oil/brine system [20]; Wang et al. used GBDT to predict the medium-term load of the power grid [21]; Zheng, Wang and others used GBDT to predict the short-term load of the power grid [22,23]. GBDT is also widely used in urban planning [24–29], life sciences [30–37], financial forecasting [38–45], energy forecasting and other fields. In urban planning work, some scholars used GBDT to predict the cooling load of low-energy buildings [26] and building energy consumption [46]. Zhang et al. proposed a GBDT-based ice storage air-conditioning cooling load forecasting model to predict air-conditioning cooling load [26]; Liu et al. used GBDT to predict Hong Kong's long-term monthly electricity demand under future climate and socioeconomic changes [47]; Zhang et al. used a GBDT-based model to predict the relationship between PM2.5 and CO2 emissions [48]; Gao et al. used GBDT to predict the carbon emissions of urban car hailing [49].

Some scholars use a variety of improved methods to optimize the performance of GBDT, forming a new method of analysis and prediction. The SPSO adaptive neural network (Sann) prediction method was proposed by Gao et al. [50], and the combination method of GBDT and DE (GBDT-DE) was proposed by Deng et al. [45]. Zhou et al. developed a learning architecture for forecasting and trading stock indices by cascading the logistic regression model to the gradient-enhanced decision tree model [42]; Zhou et al. proposed a new model that combines the gradient-enhanced decision tree with logistic regression [45]. These synthesis methods reflect the GBDT algorithm's strong compatibility and wide applicability. We found that few scholars have used the WOA algorithm to optimize the GBDT algorithm. Therefore, in this paper, we chose to use the whale algorithm to optimize GBDT, which provides a new possibility for the future optimization of GBDT.

The whale optimization algorithm (WOA) is an algorithm that was proposed by Mirjalili Seyedali in 2016, based on the behavior of whales rounding up their prey. The algorithm is inspired by the bubble-net hunting strategy. Optimization results prove that the WOA algorithm is very competitive compared to the state-of-the-art meta-heuristic algorithms as well as the conventional methods [51]. Zhuang et al. [30] used it to predict early water shortage; Wang et al. constructed a WOA-ELM model for the prediction of carbon emissions in China [52]. Zhao et al. constructed a hybrid model based on feature selection and the whale optimization algorithm (WOA) for the prediction of PM2.5 concentrations [53]. Zhao et al. proposed a WOA-LSSVM model for the prediction of CO2 emissions [54]. Yan et al. used WOA to predict evaporation in arid and humid regions of China [55]; Yang et al. optimized the algorithm based on improved ensemble empirical modal decomposition and improved the whale optimization algorithm's long- and short-term memory to predict carbon prices [56].

Many improved algorithms have been developed based on WOA. To overcome the shortcomings of low convergence accuracy and convergence speed, Yan et al. used logistic mapping to initialize population localization and improved the algorithm using inertial weighting [57]. To address the problems of the WOA algorithm's uneven population distribution, slow convergence speed and the tendency to fall into local optima, He et al. used Sobol sequences to initialize the population, a stochastic learning strategy to increase population diversity and a Corsi variance boosting algorithm to jump out of local optima to optimize the algorithm [58]. Similarly, Liu et al. introduced an optimal neighborhood perturbation strategy to solve the phenomenon of the premature algorithm [59]. Lin et al. used chaotic Tent mapping to determine the initial population position of a random generation algorithm in order to make the population distribution more uniform and speed up the convergence of the algorithm [60].

We found that various scholars use more than one optimization approach to optimize the WOA algorithm. Based on this, this paper combines multiple optimization methods to optimize the WOA algorithm in order to better improve the algorithm's optimization finding ability.

At present, the GBDT algorithm has not been widely used in carbon emission prediction. Based on this, this paper establishes the improved whale algorithm-optimized GBDT to predict China's carbon emissions.

Some of the innovations of the current study are as follows:

(1) To improve the global search ability and local search ability, this paper uses four methods: the compound chaotic map, nonlinear convergence factor, local domain perturbation and reverse learning. In addition, this paper compares the optimization performance of the algorithm and proves that the optimized whale algorithm has strong optimization ability;
(2) Based on the impact of the policy, this paper evaluates China's 2030 Carbon Peak Target, provides a scientific basis for carbon reduction policy making and puts forward relevant suggestions.

2. Materials and Methods

2.1. Standard Whale Optimization Algorithm

The specific steps of whale optimization algorithm (WOA) are discussed below.

2.1.1. Prey Encirclement Stage

Humpback whales can identify the location of prey and surround them, and WOA assumes that the current optimal candidate solution is the target prey, while the other search agents update their positions by "target prey". The formula is as follows:

$$X(i+1) = X^*(i) - A \cdot |C \cdot X^*(i) - X(i)| \quad (1)$$

$$A = 2a \cdot r_a - a \quad (2)$$

$$C = 2 \cdot r_c \quad (3)$$

where i is the current number of iterations; $X^*(i)$ is the optimal candidate solution; $X(i)$ is the current position vector; $| \ |$ is the absolute value sign; is the element-by-element multiplication; A and C are random vectors between [0, 1]; A is the convergence factor, which decreases linearly from 2 to 0.

2.1.2. Bubble-Net Attack

Humpback whales spit bubbles to attack their prey, spiraling upwards to gradually reduce the envelope to obtain food, divided into two main mechanisms of contracting the envelope and spiraling to update the position to achieve mathematical visibility. The mathematical model can be expressed as follows:

(a) Contraction of the envelope: encirclement shrinkage of the prey by means of the control parameter a of the coefficient variable A;
(b) Spiral position renewal: after encircling the prey, the whale captures it in a spiral movement, which is mathematically modelled as follows:

$$X(t+1) = X^*(t) + D_p \cdot e^{bl} cos(2\pi l) \tag{4}$$

where $D_p = |X^*(t) - X(t)|$ is the distance between the whale and its prey, b is the logarithmic spiral-shaped constant and l is a random number between $[-1, 1]$.

Humpback whales attack their prey in bubble nets in a synchronous manner with both constricted encirclement and spiral position updates. In the mathematical model, the position information is updated using the same probability and can be expressed as

$$X(t+1) = \begin{cases} X(t) - A \cdot |C \cdot X^*(i) - X(i)| & p < 0.5 \\ X(t) + D_P \cdot e^{bl} cos(2\pi l) & p \geq 0.5 \end{cases} \tag{5}$$

where p is a random number on [0, 1].

2.1.3. Searching for Prey

In addition to the bubble-net hunting strategy, humpback whales need to search for prey randomly, and the process is mathematically modeled as follows:

$$X(t+1) = X_{\text{rand}} - A \cdot |C \cdot X_{\text{rand}} - X(t)| \tag{6}$$

where X_{rand} represents a randomly selected position vector in the current population.

2.2. Modified Whale Optimization Algorithm

2.2.1. Composite Chaotic Mapping

The initial populations of most current intelligent optimization algorithms are randomly generated in the search space, and the quality of the initialized populations has a great impact on the efficiency of the optimization algorithm. WOA has the disadvantages of reducing the diversity of individuals in the late iterations and easily falling into local optima when solving problems. Chaotic operators can enhance the diversity of individuals in a population by not repeatedly traversing all states within a certain range. This paper uses Tent and Chebyshev mappings to form a composite chaotic mapping as a new search method [61].

Tent mapping is defined as:

$$x_{n+1} = 1 - 2|x_n|, -1 < x_n \leq 1 \tag{7}$$

Chebyshev mapping is defined as:

$$x_{n+1} = cos(k \cdot arccos x_n) \tag{8}$$

When the order $k \geq 2$, the interval of Chebyshev mapping is $x \in [-1, 1]$, and the non-linear factor that generates chaos is the square operation.

By embedding the standard Tent mapping into Chebyshev mapping and changing its chaotic attractor, an improved composite chaotic mapping is obtained, whose equation is

$$x_{n+1} = (cos(k \cdot (arccos(1 - |2x_n|)))) \tag{9}$$

When the order $k \geq 2$, the complex chaotic mapping interval is $x \in [-1, 1]$. The non-linear factors that generate chaos are taken as absolute values and squared operations.

2.2.2. Non-Linear Convergence Factor

In order to more effectively balance the global exploration and local exploitation performance of the algorithm, a combined convergence factor strategy is proposed in this paper.

This is specified as follows:

$$\alpha^* = \begin{cases} -0.5^{sin(\frac{\pi}{4}\alpha)} + 1 & \alpha < 0.5 \\ ln\left(20^{sin(\frac{\pi}{4}\alpha)}\right) - 1 & \alpha \geq 0.5 \end{cases} \tag{10}$$

α^* decreases nonlinearly in the [0, 2] range. The convergence factor changes more in the first period for fast convergence and less in the later period for an improvement in the local search efficiency.

2.2.3. Local Neighbourhood Perturbation

There are two modes of search in the whale algorithm, namely, search around optimal individuals and search around random individuals, both of which make it difficult for the whale algorithm to operate outside the local optimum. If it converges quickly, it is likely to fall into a local optimum.

We set up a local perturbation optimization [62] to prevent the algorithm from falling into a local optimum.

If the optimal particle in the perturbation group is better adapted than the existing global optimal particle, then the best particle in the perturbation group is better than the existing global best particle, then global best particle is assigned to the global best particle and the global best particle is used to replace the worst particle, so as to retain the existing global optimum while skipping the local optimum. The global optimal particle is assigned to the global optimal particle, and the global optimal particle replaces the worst particle.

If no better particle appears, the local perturbation is considered, the local perturbation fails and the existing particles are not changed.

2.2.4. Reverse Learning Strategy

In order to enhance the population diversity of individual whales in the search optimization process, this paper introduces a backward learning mechanism in the iterative search process of the whale algorithm. The backward learning mechanism is used to help the algorithm escape the influence of the local optimum, which is conducive to the global convergence of the algorithm.

Reverse learning is defined as follows:

Supposing $Q = (x_1, x_2, x_3, \cdots, x_n)$ is a feasible solution in an N-dimensional search space and satisfies $x_1, x_2, x_3, \cdots, x_n \in R, x_i \in [a_i, b_i]$, then its reverse solution is $Q^* = \left(x_1^*, x_2^*, x_3^*, \cdots, x_n^*\right)$, which satisfies $x_i^* = a_i + b_i - x_i, \quad i = 1, 2, \ldots, n$.

Based on this, we can see, with respect to the definition of backward learning, that there is only one corresponding backward solution for each solution in the search space. We introduce a backward learning mechanism into the whale algorithm to achieve the goal of maintaining population diversity while avoiding becoming trapped in local optimization.

2.3. Gradient Boosting Tree

GBDT was proposed by Friedman, and it mainly solves the optimization problem of general loss functions. The core idea is to fit the residuals of the previous round of base learners by the negative gradient of the loss function, so that the residual estimate of each round gradually decreases. Thus, the output of each round of the base learner gradually approximates the true value. Fitting in the negative gradient direction ensures that the loss function decreases as quickly as possible in each round of training, accelerating convergence to a local or global optimum solution.

The corresponding equation is as follows:

$$F(x, w) = \sum_{n=0}^{N} a_n h_n(x, w_n) = \sum_{n=0}^{N} f_n(x, w_m) \tag{11}$$

where x is the input sample, h is the categorical regression tree, w is the parameters of the regression tree and a denotes the weights. Solving for the optimal model (16) is equivalent to minimizing the loss function, which is:

$$F^* = arg \min_{F} \sum_{n=0}^{N} L(y_n, F(x_n, w)) \tag{12}$$

Overall, GBDT is a process of fitting the residuals and superimposing them on F. In this process, the residuals become smaller and the loss (loss function) approaches the minimum.

As GBDT is modelled with a large number of hyperparameters, the training model is not guaranteed to be optimal. In this paper, MWOA is used to optimise the four parameters of min_samples_split, min_samples_leaf, min_weight and max_depth in the GBDT model.

Explanations of these parameters are given below:

Min_samples_split specifies the minimum number of samples needed to split an internal node (not a leaf node).

Min_samples_leaf specifies the minimum number of samples to be included in each leaf node.

Min_weight_fraction_leaf specifies the minimum weight factor of the samples in a leaf node.

Max_depth specifies the maximum depth of each regression estimate. The maximum depth limits the number of nodes in the tree and this parameter is adjusted for the best performance.

2.4. MWOA-Based GBDT Prediction Model

Data are collected, and dimensionless processing is performed on the data. The gray correlation degree is applied to screen the influencing factors.

(1) Input data selection

Collect the data and do dimensionless processing on the data. Apply the gray correlation degree to screen the influencing factors.

(2) GBDT prediction model based on MWOA

On the basis of considering the influencing factors of carbon emission prediction, the MWOA-GBDT model is used to derive the energy consumption prediction results. The specific steps are as follows:

Step 1: The parameters are set and calculated to initialize the algorithm population based on Equation (9);

Step 2: The population fitness is calculated and ranked, and the current best position is recorded;

Step 3: The parameters are updated. If $p < 0.5$, one can move to Step 4, and, conversely, the searching individual attacks the prey in a spiral motion;

Step 4: If $|A| \leq 1$, the whale swims toward the optimal individual. Conversely, the whale swims toward the random individual;

Step 5: The magnitude of the fitness value between the current individual and the candidate optimal solution is used to determine whether to replace the candidate solution;

Step 6: After solving the reverse solution of the updated optimal position, the solution with the larger fitness value between them is selected as the final updated position;

Step 7: Partial disturbance is performed. The newly generated position is compared with the current optimal position and the individual fitness is compared to decide whether to replace the current optimal individual;

Step 10: It is determined whether the end condition is reached. If it has not been reached, one must return to Step 2 to continue the iteration.

Finally, the parameters obtained from the optimization in MWOA as previously described are assigned to GBDT to complete the prediction.

The whole model is shown in Figure 1.

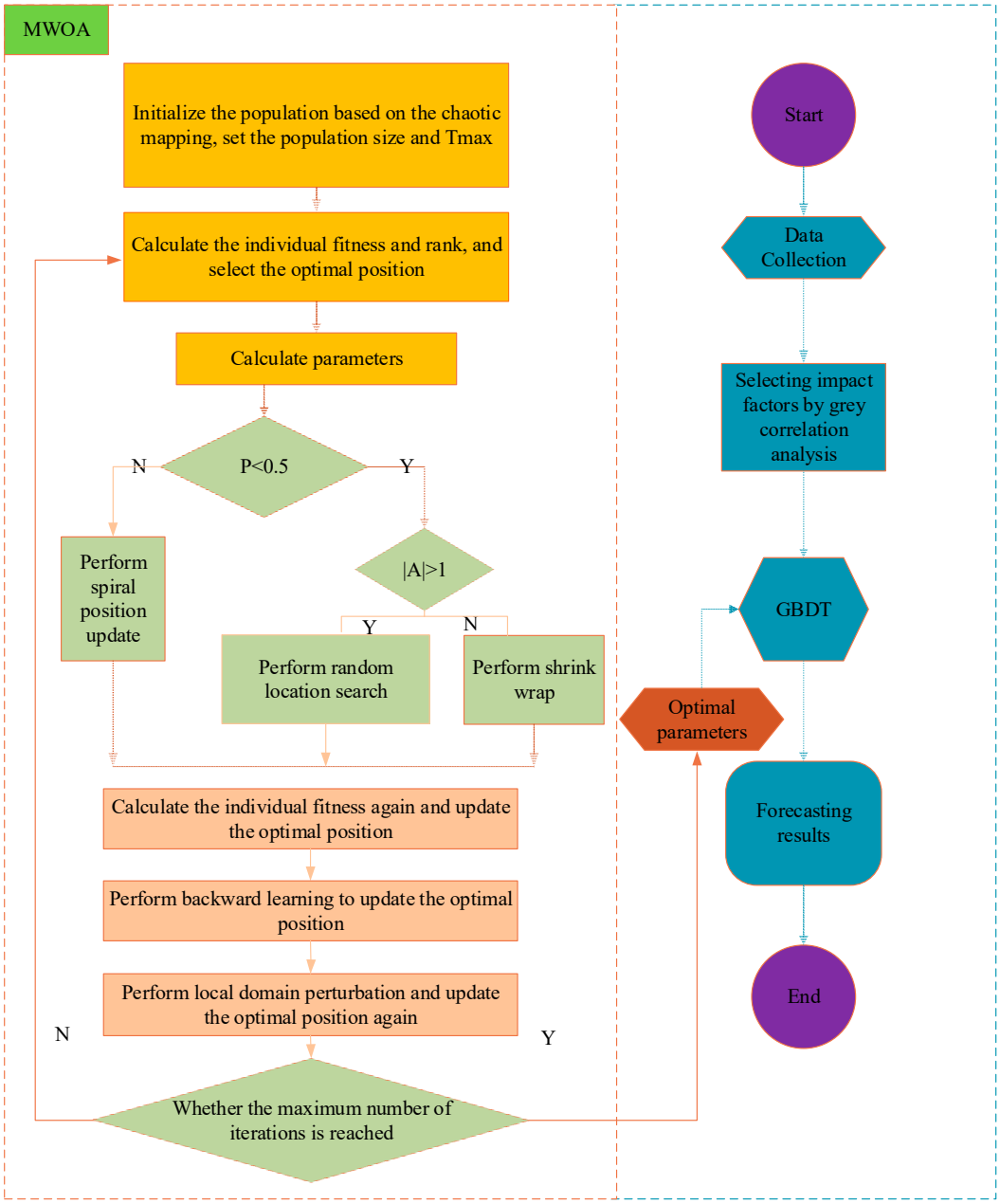


Figure 1. The prediction process of the model.

3. Experimental Analysis

3.1. Confirmation of Input Values for the Prediction Model

There are many factors influencing carbon emissions, and we chose to select China's total GDP, residential consumption level, total import and export, industrial structure, urbanization rate and total energy consumption from 1990 to 2019 as initial values based on some past studies and experience (data from the World Bank, China Carbon Accounting Database and BP Energy Statistical Yearbook).

In order to determine the main influencing factors more accurately and exclude the influence of secondary factors, we used gray correlation analysis to determine the final influencing factors.

The analysis results of this paper are shown in the following table.

In Table 1, we selected influences with a correlation of 0.7 or higher as input values for the prediction model.

Table 1. Grey correlations.

Impact Factor	Grey Correlation
GDP (RMB 100 million)	0.70810
Resident consumption level (RMB)	0.70908
Total imports and exports (RMB billion)	0.71578
Industry structure (%)	0.73538
Energy consumption structure (%)	0.68754
Population (10,000 people)	0.65347
Urbanization rate (%)	0.75202
Total energy consumption (10^4 tce)	0.96839

Based on the above, we chose GDP, population consumption level, total import and export, urbanization rate and total energy consumption from 1990 to 2019 as the data set for this experiment.

3.2. MWOA-GBDT-Based Carbon Emission Forecasting in China

In this paper, the K-fold cross-validation method was used to prevent the overfitting of the model on the test set. The data from 1990 to 2010 were divided into training and validation sets, the verification set at a ratio of 4:1 and the remaining sample data from 2010 to 2019 were used as the test set. Each time, we used the five groups of sample data as the training data and the remaining group of sample data as the verification set for a total of five times, in order to use the average accuracy to verify the model. As the sample data in this study are small, we adopted five-fold cross-validation for every model, in which each group had four samples. The training set had 16 samples and the validation set has 4 samples.

The simulations were run on an Inter(R) Core(TM) CUP: i7-9750H, 16 GB RAM, 2.60 GHz main frequency computer, and the program was implemented using Python programming. The population size was set to 30.

The algorithm parameters are set as shown in Table 2, where the first decimal of each parameter is rounded to the nearest whole number.

Table 2. Parameter settings related to the GBDT algorithm.

Metrics	Range
min_samples_split	[1, 10]
min_samples_leaf	[1, 10]
min_weight_fraction_leaf	[0, 0.5]
max_depth	[1, 10]

The predicted results are shown in the graph below.

Relative error (RE) refers to the absolute error caused by the measurement and the ratio of the measured (agreed) true value multiplied by 100% of the resulting value, expressed as a percentage. The closer the RE value is to 0, the better the variables of the equation explain y and the better the model fits the data. The closer the RE value is to 1, the worse the model fits.

In general, the relative error is more reflective of the degree of confidence in the measurement. The actual values for the period of 1990–2019 are compared with the predicted values predicted using MWOA-GBDT, as shown in Table 3 and Figure 2.

Table 3. Table of relative errors.

Year	Actual Value (Million Tons)	Predicted Value (Million Tons)	RE (%)
1990	2088.854238	2090.273265	0.07%
1991	2200.885206	2201.585453	0.03%
1992	2295.775295	2296.007805	0.01%
1993	2500.729949	2500.970731	0.01%
1994	2599.5029	2599.938564	0.02%
1995	2900.265046	2895.900413	0.15%
1996	2871.980724	2876.946359	0.17%
1997	2925.748702	2924.439849	0.04%
1998	3020.716711	3017.665887	0.10%
1999	2920.896797	2923.52852	0.09%
2000	3099.685154	3101.90848	0.07%
2001	3255.951126	3255.92946	0.00%
2002	3511.727723	3511.81841	0.00%
2003	4068.094745	4068.242272	0.00%
2004	4741.830883	4741.818747	0.00%
2005	5407.51803	5407.501885	0.00%
2006	5961.808473	5961.646666	0.00%
2007	6473.211479	6473.05578	0.00%
2008	6669.111668	6669.091118	0.00%
2009	7131.511865	7131.449172	0.00%
2010	7830.968904	7830.918884	0.00%
2011	8569.652812	8569.504519	0.00%
2012	8818.41331	8818.224146	0.00%
2013	9188.380792	9185.842412	0.03%
2014	9116.341237	9118.100151	0.02%
2015	9093.303762	9093.147602	0.00%
2016	9054.476007	9054.255438	0.00%
2017	9245.581695	9245.049652	0.01%
2018	9606.6	9605.988844	0.01%
2019	9920.5	9919.274747	0.01%

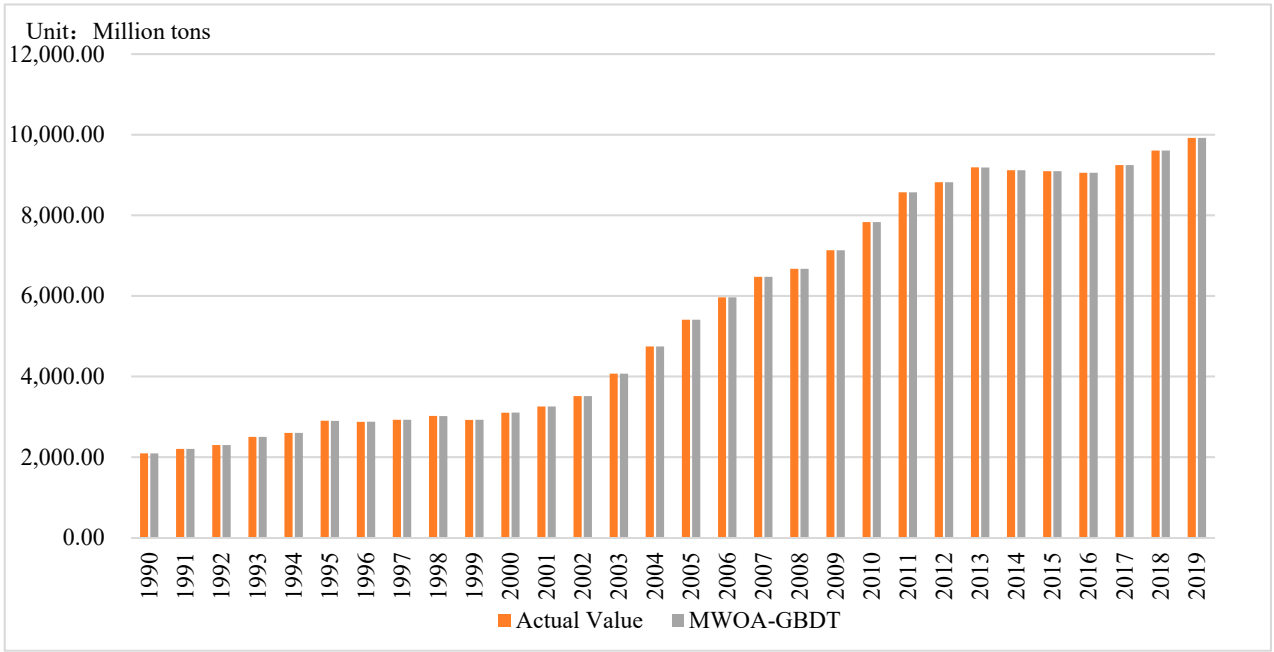


Figure 2. Comparison of prediction results.

As can be seen from the above graphs, the prediction curves for energy consumption formed using the MWOA-GBDT model show an excellent fit to the actual curves and the predictions are quite significant, with the relative error at all prediction points not even exceeding 1%. This proves that MWOA-GBDT has superior prediction performance.

3.3. Comparison of Prediction Results between Models

In order to further demonstrate the reliability of MWOA-GBDT prediction models, we selected five models (WOA-GBDT, PSO-GBDT, GWO-GBDT, BA-GBDT and GBDT) to predict the data via the same samples, and the prediction results and prediction errors of each model are analyzed and studied in this paper. Figure 3 shows the actual carbon emission values and the predicted carbon emission values of each model.

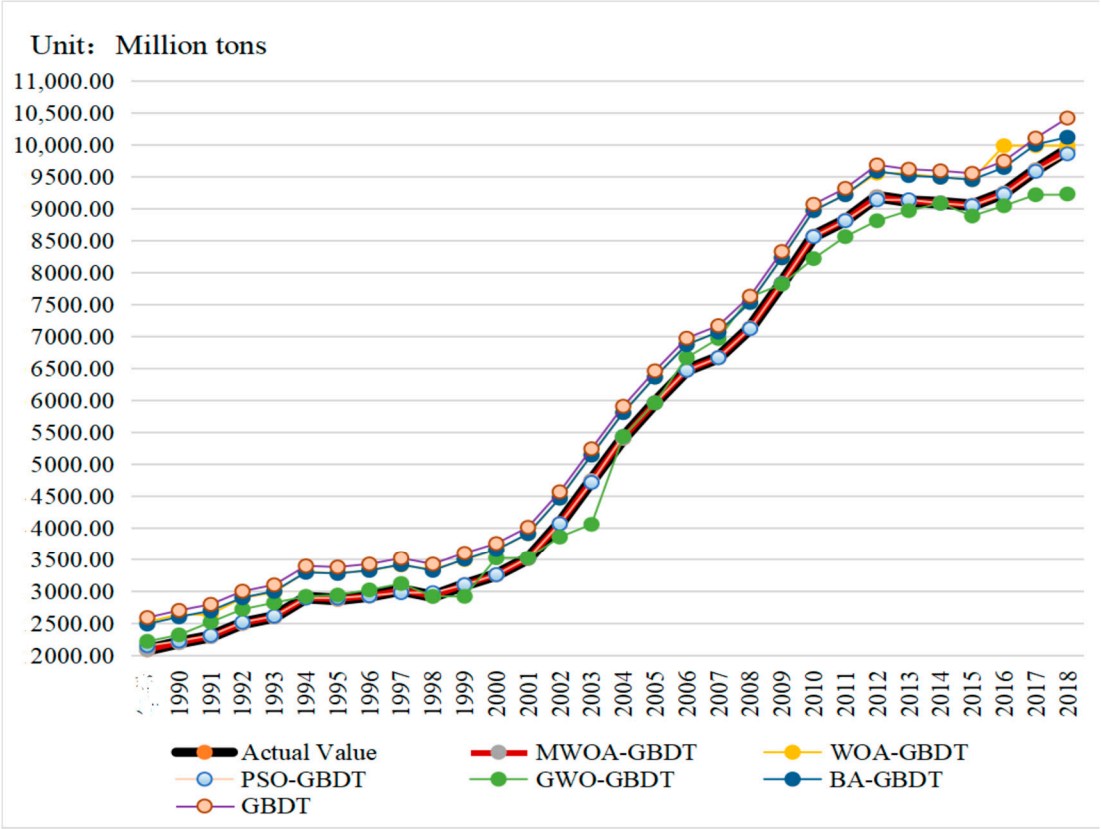


Figure 3. Comparison of model prediction results.

The prediction results of the MWOA-GBDT model fit the actual carbon emission values best, and the fitting effect of PSO-GBDT is also very significant. The prediction results of GWO-GBDT have large fluctuation, and the prediction results of GBDT have an obvious error. The box plots in the figure show the minimum, first quartile, median, third quartile and maximum values of the relative errors in the six models.

Figures 4 and 5 compare the relative error magnitudes of the models. As seen in Figure 4, the MWOA-GBDT model has the smallest prediction error, followed by PSO-GBDT.

In addition to visually comparing the magnitude and distribution of errors, MAPE (mean absolute percentage error), RMSE (root mean square error) and MAE (mean absolute error) were used to compare the forecasting accuracy. The metrics selected by us are formulated as follows:

$$MAPE = \frac{1}{n}\sum_{i=1}^{n}\left|\frac{\hat{y}_i - y_i}{y_i}\right| \quad (13)$$

$$RMSE = \sqrt{\frac{1}{n}\sum_{i=1}^{n}(\hat{y}_i - y_i)^2} \quad (14)$$

$$MAE = \frac{1}{n}\sum_{i=1}^{n}|\hat{y}_i - y_i| \quad (15)$$

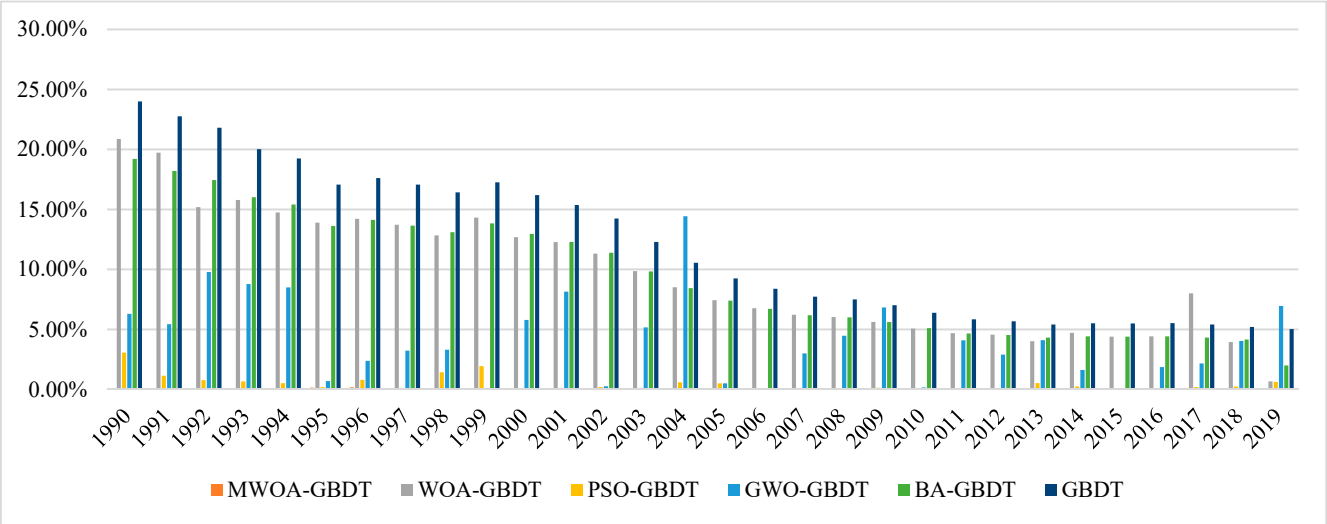


Figure 4. Relative error plots for the six models.

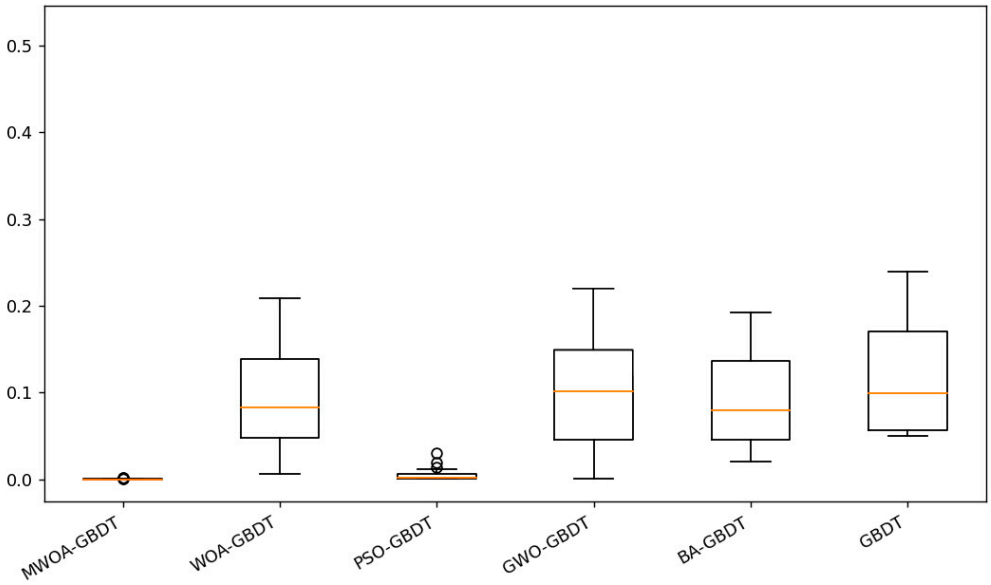


Figure 5. Model error box line diagram.

MAPE is an indicator that represents the average deviation of the predicted outcome from the true outcome. MAPE takes into account not only the error between the predicted and true values, but also the ratio between the error and the true value. In addition, MAPE can also evaluate the goodness of the model.

The indicator RMSE represents the deviation of the observed value from the true value.

The indicator MAR represents the average of the absolute values of the deviations of the predicted values from the true values.

The smaller the value of these three indicators, the better the accuracy of the prediction model in describing the experimental data.

As we can see from Table 4, among the three indicators MAPE, RMSE and MAR, MWOA-GBDT has the smallest value, which proves that the model accuracy is relatively optimal. It is closely followed by PSO-GBDT, and the unoptimized GBDT has the relatively worst prediction accuracy.

Table 4. Calculation results.

	MWOA-GBDT	PSO-GBDT	BA-GBDT	GWO-GBDT	WOA-GBDT	GBDT
MAPE (%)	0.028	0.546	0.484	0.512	1.854	1.90
RMSE (Million tons)	1.64	88.71	26.24	85.34	4770.59	4863.45
MAR (Million tons)	0.99	5.69	4.32	5.26	3874.14	3980.81

4. China's Carbon Emission Projections for 2020–2035

China has proposed to achieve the "carbon peak" target by 2030, and, therefore, this paper uses MWOA-GBDT to project carbon emission values for 2020–2035 to help China formulate relevant policies. In addition to the carbon peak target, at the UN Climate Ambition Summit, President Xi announced that, by 2030, China's carbon emissions intensity will drop by more than 65% compared to 2005.

Based on this, this paper uses MWOA-GBDT to project China's carbon emissions and carbon intensity data for 2020–2035 in conjunction with existing policies and data to determine whether China will be able to efficiently meet its carbon peaking targets.

4.1. Simulation of Influencing Factors

Before predicting China's carbon emissions, it is necessary to forecast the influencing factors in advance. Since China has only proposed carbon neutrality and carbon peaking targets come 2020, a considerable number of important policies have been or are being introduced. The traditional gray forecasting method is based on the past situation, and it does not match with the impact factors that we need. Therefore, it is necessary to combine the factors with China's policy planning to determine the trend of some influencing factors, and then combine them with the gray forecasting method to obtain more accurate forecasting results. In this paper, all of the indicators are set according to China's current plans and targets.

4.1.1. GDP

Due to the COVID-19 pandemic, the GDP growth rate for 2020 is 2.3% per year. At China's two sessions, China set its expected GDP growth target for 2021 at 6% or more. The Fifth Plenary Session of the 19th Central Committee proposed that GDP per capita should reach the level of medium developed countries by 2035, implying that China's GDP growth rate needs to be maintained in a reasonable range over the next 15 years. In the process of shifting from high growth to high quality development, China's total economic base is increasing in size, while the potential economic growth rate is expected to slow down due to declining labor productivity growth and demographic changes, and then the GDP growth rate will gradually decline over time.

4.1.2. Consumption Level of the Population

Under the influence of the COVID-19 pandemic, residents' consumption levels have dropped; however, under the joint promotion of policy support factors, such as a stable employment situation and recovery of business activities due to economic recovery and continuous increase in livelihood protection, residents' disposable income has improved in tandem with the economic situation. In the long run, the 14th Five-Year Plan period will be a critical period for China to move towards becoming a high-income country. The Fifth Plenary Session of the 19th CPC Central Committee clearly put forward that raising

people's income level is a very important issue. We will strive to reach a new level of livelihood and well-being, with the growth of people's income and economic growth essentially synchronized and the distribution structure significantly improved. In the future, China's economic upward growth pulling force will mainly rely on consumer demand, which mainly requires raising residents' income, and better income distribution can improve overall consumer demand and raise residents' consumption level.

4.1.3. Total Imports and Exports

China's Ministry of Commerce in July in the "14th Five-Year Plan" for business development proposed that, by 2025, China's total imports and exports of goods should increase from USD 4.65 trillion in 2020 to USD 5.1 trillion, with an average annual growth rate of 2%. Officials have indicated that China will expand imports of high-quality consumer goods, advanced technology, important equipment and energy resources, and improve the quality of exports. The global target of "double carbon" will also greatly enhance the global competitiveness of China's manufacturing industry and improve the country's export capacity. However, the continued evolution of the overseas COVID-19 pandemic has exacerbated the complexity of the foreign trade situation and put pressure on future import and export trade.

4.1.4. Industrial Structure

At present, the industrial base of China's service industry trade development is still relatively weak, and the share of the service industry in the value added of GDP is 54.5%, which is lower than the share of world service industry in the value added of the world GDP of 67%. Under the double carbon target, China will prevent the continued development of high energy-consuming and high-emission industries and accelerate the development of strategic emerging industries, high-tech industries and modern service industries. As a result, the share of the service sector will increase until it reaches the world average.

4.1.5. Urbanization Rate

The integration of peak carbon and carbon neutrality with urbanization is proceeding in an orderly manner. Globally, the countries and regions that have already achieved peak carbon and that are promoting carbon neutrality are generally developed countries and regions. The common feature of these developed countries and regions is that they have already achieved urbanization. In a certain sense, they are building low-carbon and zero-carbon cities in the post-urbanization and post-industrialization period. The difference in China is that urbanization has not yet been completed and is still in the process of shaping changes, which provides a scenario where carbon peaking and carbon neutrality can be fully utilized, and each city needs to target its urbanization process according to its own carbon pressure. During the 2030–2035 period, China's resident population urbanization rate is also expected to approach or reach its peak and enter a relatively stable state.

4.1.6. Total Energy Consumption

In the future, because China is still a developing country, China's total energy consumption will remain on the increase for a longer period of time, and the growth rate of energy consumption is expected to show a gradual slowdown. The government's work report proposes that energy consumption per unit of GDP will be reduced by 13.5% during the 14th Five-Year Plan period. The National Development and Reform Commission (NDRC) has proposed a target of controlling total energy consumption to within six billion tonnes of standard coal by 2030. With the continuous development of high-tech carbon reduction technologies and policy subsidies, the total energy consumption will continue to decrease in later years. At present, China is entering the late stages of industrialization and the overall energy consumption demand has seen a post-peak decline. The World and China Energy Outlook 2050, published in 2016, states that China's energy consumption will peak at around 2035 under the influence of accelerated economic restructuring and

policies to control total energy consumption. Based on the current new mission targets and new energy policies, total energy consumption is expected to peak by 2030.

Based on the above, we combined policy regulations and the gray forecasting method to obtain the data on influencing factors in China for the period of 2020–2035.

4.2. Forecast Results

Based on our previous settings of the corresponding influencing factors, we used the constructed MWOA-GBDT model to forecast the carbon emission values of China for the period of 2020–2035. The prediction results are shown in Figure 6 and Table 5 and the comparison results of the predictions are shown in Table 6.

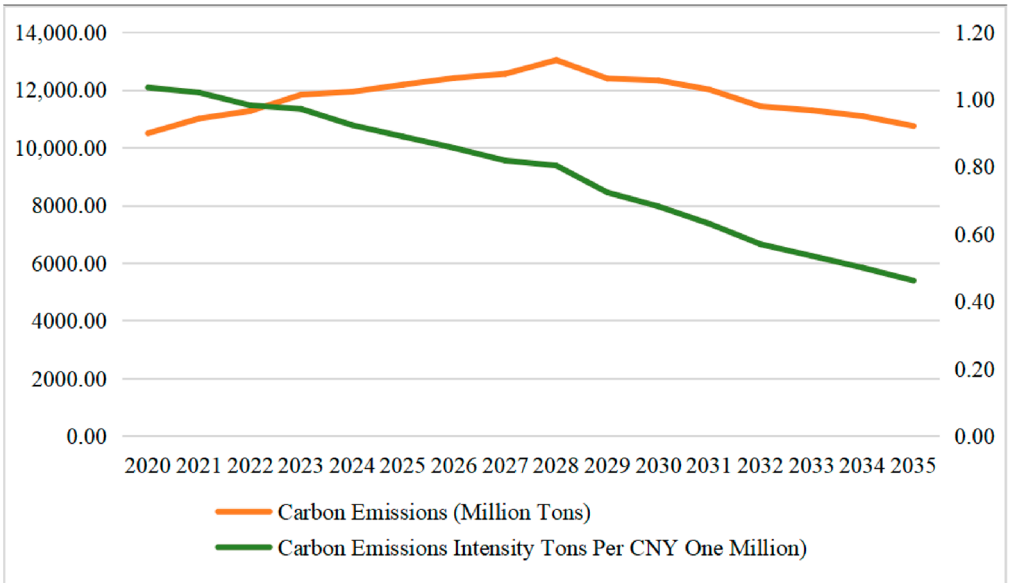


Figure 6. Trend graph of predicted results.

Table 5. Forecast results.

Year	Carbon Emissions (Million Tons)	Carbon Emissions Intensity Tons Per CNY One Million
2020	11,126.69642	1.097680814
2021	11,431.2639	1.059894057
2022	11,744.00943	1.024356985
2023	12,065.095	0.99092588
2024	12,394.67921	0.959467641
2025	12,732.91655	0.929858935
2026	12,947.38987	0.892843706
2027	13,299.93001	0.866875849
2028	13,435.77832	0.82850549
2029	13,285.61181	0.775800761
2030	13,196.19702	0.730407079
2031	13,138.33327	0.689947183
2032	12,848.25022	0.640753794
2033	12,566.72413	0.595735585
2034	12,293.38063	0.554498114
2035	12,027.83171	0.516686112

Table 6. Forecast results.

Year	Carbon Emissions (Million Tons)	Carbon Emissions Intensity (Tons per CNY One Million)	Can We Achieve Our Carbon Peak Target?	Can Carbon Intensity Targets be Met?
2020	11,126.69642307	1.09768081375886	—	—
2030	13,196.19701519	0.7304070790301	Yes	Yes
2035	12,027.83170639	0.516686112487781	—	—

Carbon intensity refers to the amount of carbon dioxide emissions per unit of GNP growth. This indicator is used to measure the relationship between a country's economy and its carbon emissions. If a country's economic growth is accompanied by a decline in carbon dioxide emissions per unit of GNP, then the country has achieved a low carbon development model. The predicted results are shown in Table 6. To show more clearly the trend of carbon emission values and carbon emission intensity, a line graph is drawn in this paper, as shown in Figure 6.

As can be seen in Figure 6, the carbon emission values show an increasing and then decreasing trend, peaking in 2028, while the carbon emission intensity shows a decreasing trend year by year. The comparison of the results in Table 6 shows that both policy target values for China can be achieved under the existing policies, while the peak carbon target will be achieved earlier in 2028.

5. Conclusions and Recommendations

Based on the results in the previous subsection, the following conclusions can be drawn in this paper.

(1) Total energy consumption, urbanization level and industrial structure are the top three factors with the highest correlation. Therefore, relevant suggestions can be made in terms of low carbon consumption to further reduce carbon emissions;
(2) By comparing the performance of the optimization algorithm and the prediction model, the MWOA-GBDT model constructed in this paper has an excellent prediction capability;
(3) Due to the superiority of MWOA-GBDT in error comparisons, the prediction results of carbon emission consumption have practical significance. According to the prediction results of 2020–2035, China can achieve the carbon emission-related target in 2030 under the existing policies.

To ensure that China's carbon targets are met on time, this paper also makes the following observations.

As China is currently in a period of high-quality development, many high-energy consumption and high-carbon projects are still being deployed, and the Fifth Plenary Session of the 19th CPC Central Committee has put forward a clear requirement to "formulate a carbon emission peaking action plan by 2030". It is necessary to make some relevant recommendations.

The recommendations in this paper are as follows:

(1) Acceleration of the adjustment of industrial structure and implementation of industry transformation.

China's high-carbon industries account for more than 70% of total energy consumption. From the screening of the above-mentioned influencing factors, there is a close connection between industrial structure and energy consumption. Strictly controlling the new production capacity of high energy-consuming industries and promoting the transformation and upgrading of traditional high energy-consuming industries are the key measures to reduce the value of carbon emissions.

(2) Acceleration of the construction of a perfect carbon market system.

Building a national carbon emission trading market is an important institutional innovation to control greenhouse gas emissions and promote green and low-carbon de-

velopment using market mechanisms, and it has become one of the core policy tools to achieve China's peak CO2 emission target and implement carbon-neutral vision.

(3) Building a clean, low-carbon, safe and efficient energy system.

Carbon dioxide emissions from energy consumption account for nearly 90% of China's total carbon dioxide emissions, and total energy consumption is highly correlated with the value of carbon emissions. Promoting the effective allocation and utilization of energy resources and effectively improving the energy-saving technology and energy management capacity of key energy-using enterprises are important tasks.

(4) Promotion of a carbon-labeling system for products and low-carbon consumption by the public.

On the basis of setting mandatory product energy efficiency standards, the state can establish a product energy efficiency rating and certification system to compel enterprises to express the effectiveness and level of product energy efficiency levels on product packaging, which can effectively guide consumers' demand and purchase behavior.

In summary, we forecasted China's future carbon emissions for the sake of its future policy development and made some relevant recommendations based on the current situation.

Author Contributions: X.C.: conceptualization, methodology and writing—original draft preparation; S.E. and D.N.: data curation, analysis, and writing—original draft preparation; B.C. and J.F.: resources, investigation, and validation. All authors have read and agreed to the published version of the manuscript.

Funding: This work is supported by Theory and Method of Collaborative Data Space Design for Manufacturing Multi-value Chain, National Key R&D Program of China (2020YFB1707800).

Data Availability Statement: The data presented in this study are available upon request from the corresponding author. The data are not publicly available due to privacy reasons.

Conflicts of Interest: The authors declare no conflict of interest.

References

1. Zhao, X.M.; Wei, X. A study on the relationship between traditional energy prices and carbon trading prices in China—Based on panel data of seven pilot provinces and cities of carbon trading in China. *Ecol. Econ.* **2019**, *35*, 31–34.
2. Kazuya, N.; Chisato, T.; Shigehiro, I.; Shoji, H. Tree manipulation experiment for the short-term effect of tree cutting on N2O emission: A evaluation using Bayesian hierarchical modeling. *Environ. Pollut.* **2021**, *288*, 117725.
3. Tamim, N.; Laboureur, D.M.; Hasan, A.R.; Mannan, M.S. Developing leading indicators-based decision support algorithms and probabilistic models using bayesian network to predict kicks while drilling. *Process Saf. Environ.* **2018**, *121*, 239–246. [CrossRef]
4. Alade, I.O.; Rahman, M.A.; Saleh, T.A. Predicting the specific heat capacity of alumina/ethylene glycol nanofluids using support vector regression model optimized with bayesian algorithm. *Sol. Energy* **2019**, *183*, 74–82. [CrossRef]
5. Lee, D.H.; Kim, K.J. Optimizing Mean and Variance of Multiresponse in a Multistage Manufacturing Process Using a Patient Rule Induction Method. *Procedia Manuf.* **2019**, *39*, 618–624. [CrossRef]
6. Liu, Y.; Hu, X.; Luo, X.; Zhou, Y.; Farah, S. Identifying the most significant input parameters for predicting district heating load using an association rule algorithm. *J. Clean. Prod.* **2020**, *275*, 122984. [CrossRef]
7. Du, P.; Cao, S.; Li, Y. Predicting protein subchloroplast locations with pseudo-amino acid composition and the evidence-theoretic K-nearest neighbor (ET-KNN) algorithm. *J. Theor. Biol.* **2009**, *261*, 330–335. [CrossRef] [PubMed]
8. Jung, J.; Kim, S.; Hong, S.; Kim, K.; Kim, E.; Im, J.; Heo, J. Effects of national forest inventory plot location error on forest carbon stock estimation using k-nearest neighbor algorithm. *ISPRS J. Photogramm.* **2013**, *81*, 82–92. [CrossRef]
9. Goodrich, J.P.; Wall, A.M.; Campbell, D.I.; Fletcher, D.; Wecking, A.R.; Shipper, L.A. Improved gap filling approach and uncertainty estimation for eddy covariance N_2O fluxes. *Agric. For. Meteorol.* **2021**, *297*, 108280. [CrossRef]
10. Zolfaghari, A.A.; Taghizadeh-Mehrjardi, R.; Moshki, A.R.; Malone, B.P.; Weldeyohannes, A.O.; Sarmadian, F.; Yazdani, M.R. Using the nonparametric k-nearest neighbor approach for predicting cation exchange capacity. *Geoderma* **2016**, *265*, 111–119. [CrossRef]
11. Tso, G.K.F.; Yau, K.K.W. Predicting electricity energy consumption: A comparison of regression analysis, decision tree and neural networks. *Energy* **2007**, *32*, 1761–1768. [CrossRef]
12. Nie, P.; Roccotelli, M.; Fanti, M.P.; Ming, Z.; Li, Z. Prediction of home energy consumption based on gradient boosting regression tree. *Energy Rep.* **2021**, *7*, 1246–1255. [CrossRef]

13. Wy, A.; Szbc, D. Using decision tree analysis to identify the determinants of residents' CO 2 emissions from different types of trips: A case study of Guangzhou, China. *J. Clean. Prod.* **2020**, *277*, 124071.
14. Wang, M.X. A review of data mining. *Softw. Guid.* **2013**, *12*, 135–137.
15. Friedman, J.H. Greedy function approximation: A gradient boosting machine. *Ann. Stat.* **2001**, *29*, 1189–1232. [CrossRef]
16. Zhang, C.S.; Liu, C.C.; Zhang, X.L.; George, A. An up-to-date comparison of state-of-the-art classification algorithms. *Expert Syst. Appl.* **2017**, *82*, 128–150. [CrossRef]
17. Fan, J.; Yue, W.; Wu, L.; Zhang, F.; Cai, H.; Wang, X.; Lu, X.; Xiang, Y. Evaluation of SVM, ELM and four tree-based ensemble models for predicting daily reference evapotranspiration using limited meteorological data in different climates of China. *Agric. For. Meteorol.* **2018**, *263*, 225–241. [CrossRef]
18. Lu, X.; Ju, Y.; Wu, L.; Fan, J.; Zhang, F.; Li, Z. Daily pan evaporation modeling from local and cross-station data using three tree-basedmachine learning models. *J. Hydrol.* **2018**, *566*, 668–684. [CrossRef]
19. David, M.; Luis, M.A.; Lauret, P. Comparison of intraday probabilistic forecasting of solar irradiance using only endogenous data. *Int. J. Forecast.* **2018**, *34*, 529–547. [CrossRef]
20. Amar, M.N.; Shateri, M.; Hemmati-Sarapardeh, A.; Alamatsaz, A. Modeling oil-brine interfacial tension at high pressure and high salinity conditions. *J. Petrol. Sci. Eng.* **2019**, *183*, 106413. [CrossRef]
21. Wang, S.M.; Wang, S.X.; Wang, D. Combined probability density model for medium term load forecasting based on quantile regression and kernel density estimation. *Energy Procedia* **2019**, *158*, 6446–6451. [CrossRef]
22. Zheng, K.W.; Yang, C. Research on short-term load forecasting based on iterative decision tree (GBDT). *Guizhou Electr. Power Tech.* **2017**, *20*, 82–84.
23. Wang, H.Y.; Yang, C.; Tang, H. Research on GBDT short-term load forecasting based on LightGBM improvement. *Automat. Instrum.* **2018**, *39*, 76–78+82.
24. Ma, J.; Cheng, J.C.P. Identification of the numerical patterns behind the leading counties in the U.S. local green building markets using data mining. *J. Clean. Prod.* **2017**, *151*, 406–418. [CrossRef]
25. Park, H.; Haghani, A.; Samuel, S.; Knodler, M.A. Real-time prediction and avoidance of secondary crashes under unexpected traffic congestion. *Accid. Anal. Prev.* **2018**, *112*, 39–49. [CrossRef] [PubMed]
26. Zhang, W.; Yu, J.; Zhao, A.; Zhou, X. Predictive model of cooling load for ice storage air-conditioning system by using GBDT. *Energy Rep.* **2021**, *7*, 1588–1597. [CrossRef]
27. Wang, R.; Lu, S.L.; Feng, W. A three-stage optimization methodology for envelope design of passive house considering energy demand, thermal comfort and cost. *Energy* **2020**, *192*, 11672314. [CrossRef]
28. Wu, Z.; Zhou, Y.; Wang, H.; Jiang, Z. Depth prediction of urban flood under different rainfall return periods based on deep learning and data warehouse. *Sci. Total Environ.* **2020**, *716*, 137077. [CrossRef]
29. Tang, T.; Liu, R.; Choudhury, C. Incorporating weather conditions and travel history in estimating the alighting bus stops from smart card data. Sustain. *Cities Soc.* **2019**, *53*, 101927. [CrossRef]
30. Zhuang, S.; Wang, P.; Jiang, B.; Li, M.; Gong, Z. Early detection of water stress in maize based on digital images. *Comput. Electron. Agric.* **2017**, *140*, 461–468. [CrossRef]
31. Jia, C.; Yang, Q.; Zou, Q. NucPosPred: Predicting species-specific genomic nucleosome positioning via four different modes of general PseKNC. *J. Theor. Biol.* **2018**, *450*, 15–21. [CrossRef] [PubMed]
32. Dai, W.; Jin, H.; Zhang, Y.; Liu, T.; Zhou, Z. Detecting temporal changes in the temperature sensitivity of spring phenology with global warming: Application of machine learning in phenological model. *Agric. For. Meteorol.* **2019**, *279*, 107702. [CrossRef]
33. Yang, Q.; Jia, C.; Li, T. Prediction of aptamer–protein interacting pairs based on sparse autoencoder feature extraction and an ensemble classifier. *Math. Biosci.* **2019**, *11*, 103–108. [CrossRef]
34. Zhou, S.; Wang, S.; Wu, Q.; Azim, R.; Li, W. Predicting potential miRNA-disease associations by combining gradient boosting decision tree with logistic regression. *Comput. Biol. Chem.* **2020**, *85*, 107200. [CrossRef] [PubMed]
35. Huan, J.; Li, H.; Li, M.B.; Chen, B. Prediction of dissolved oxygen in aquaculture based on gradient boosting decision tree and long short-term memory network: A study of Chang Zhou fishery demonstration base. *Comput. Electron. Agric.* **2020**, *175*, 105530. [CrossRef]
36. Ghosh, S.; Maulik, S.; Chatterjee, S.; Mallick, I.; Chakravorty, N.; Mukherjee, J. Prediction of survival outcome based on clinical features and pretreatment 18fdg-pet/ct for hnscc patients. *Comput. Methods Prog. Biomed.* **2020**, *195*, 105669. [CrossRef]
37. Yu, P.; Gao, R.; Zhang, D.; Liu, Z.P. Predicting coastal algal blooms with environmental factors by machine learning methods. *Ecol. Indic.* **2021**, *123*, 107334. [CrossRef]
38. Wl, A.; Hong, F.A.; Min, X.B. Step-wise multi-grained augmented gradient boosting decision trees for credit scoring. *Eng. Appl. Artif. Intell.* **2021**, *97*, 104036.
39. Li, Y.W.; Wang, X.Y.; Che, C.C.; Jing, C.Y.; Wu, T. Exploring firms' innovation capabilities through learning systems. *Neurocomputing* **2020**, *409*, 27–34. [CrossRef]
40. Du, X.D.; Li, W.; Ruan, S.M.; Li, L. Cus-heterogeneous ensemble-based financial distress prediction for imbalanced dataset with ensemble feature selection. *Appl. Soft Comput.* **2020**, *97*, 106758. [CrossRef]
41. Yang, J.S.; Zhao, C.Y.; Yu, H.T.; Chen, H.Y. Use GBDT to predict the stock market. *Procedia Comput. Sci.* **2020**, *174*, 161–171. [CrossRef]

42. Zhou, F.; Zhang, Q.; Sornette, D.; Jiang, L. Cascading logistic regression onto gradient boosted decision trees for forecasting and trading stock indices. *Appl. Soft Comput.* **2019**, *84*, 105747. [CrossRef]
43. Zhou, J.; Li, W.; Wang, J.X.; Ding, S.; Xia, C.Y. Default prediction in p2p lending from high-dimensional data based on machine learning. *Phys. A* **2019**, *534*, 122370. [CrossRef]
44. Zhang, H.B.; Zhong, H.; Bai, W.H.; Pan, F. Cross-platform rating prediction method based on review topic. *Future Gener. Comput. Syst.* **2019**, *101*, 236–245. [CrossRef]
45. Deng, S.K.; Wang, C.G.; Wang, M.Y.; Sun, Z. A gradient boosting decision tree approach for insider trading identification: An empirical model evaluation of china stock market. *Appl. Soft Comput.* **2019**, *83*, 105652. [CrossRef]
46. Wang, R.; Lu, S.; Li, Q. Multi-criteria comprehensive study on predictive algorithm of hourly heating energy consumption for residential buildings. *Sustain. Cities Soc.* **2019**, *49*, 101623. [CrossRef]
47. Liu, S.; Zeng, A.; Lau, K.; Ren, C.; Chan, P.; Ng, E. Predicting long-term monthly electricity demand under future climatic and socioeconomic changes using data-driven methods: A case study of Hong Kong. *Sustain. Cities Soc.* **2021**, *70*, 102936. [CrossRef]
48. Zhang, T.N.; He, W.H.; Zheng, H.; Cui, Y.P.; Song, H.Q.; Fu, S.L. Satellite-based ground PM2.5 estimation using a gradient boosting decision tree. *Chemosphere* **2021**, *268*, 128801. [CrossRef] [PubMed]
49. Jiong, G.J.; Ma, S.F.; Peng, B.B.; Zuo, J.; Du, H.B. Exploring the nonlinear and asymmetric influences of built environment on CO_2 emission of ride-hailing trips. *Environ. Impact Asses.* **2021**, *92*, 106691.
50. Gao, Y.N.; Li, Q.; Wang, S.S.; Gao, J.F. Adaptive neural network based on segmented particle swarm optimization for remote-sensing estimations of vegetation biomass. *Remote Sens. Environ.* **2018**, *211*, 248–260. [CrossRef]
51. Mirjalili, S.; Lewis, A. The whale optimization algorithm. *Adv. Eng. Softw.* **2016**, *95*, 51–67. [CrossRef]
52. Wang, K.K.; Niu, D.X.; Zhen, H.; Sun, L.J.; Xu, X.M. A Study on Carbon Emission Forecasting in China Based on WOA-ELM Model. *Ecol. Econ.* **2020**, *36*, 20–27.
53. Zhao, F.; Li, W. A combined model based on feature selection and woa for pm2.5 concentration forecasting. *Atmosphere* **2019**, *10*, 223. [CrossRef]
54. Zhao, H.R.; Guo, S.; Zhao, H.R. Energy-Related CO2 Emissions Forecasting Using an Improved LSSVM Model Optimized by Whale Optimization Algorithm. *Energies* **2017**, *10*, 874. [CrossRef]
55. Yan, Z.; Sha, J.; Liu, B.; Tian, W.; Lu, J. An ameliorative whale optimization algorithm for multi-objective optimal allocation of water resources in handan, china. *Water* **2018**, *10*, 87. [CrossRef]
56. Yan, S.C.; Wu, L.F.; Fan, J.L.; Zhang, F.C.; Zou, Y.F.; Wu, Y. A novel hybrid WOA-XGB model for estimating daily reference evapotranspiration using local and external meteorological data: Applications in arid and humid regions of China. *Agric. Water Manag.* **2021**, *244*, 106594. [CrossRef]
57. Yang, S.M.; Chen, D.J.; Li, S.L.; Wang, W.J. Carbon price forecasting based on modified ensemble empirical mode decomposition and long short-term memory optimized by improved whale optimization algorithm. *Sci. Total Environ.* **2020**, *716*, 137117. [CrossRef]
58. He, Q.; Wei, K.Y.; Xu, Q.S. A whale optimization algorithm based on hybrid policy improvement. *Comput. Appl. Res.* **2019**, *36*, 6.
59. Liu, L.; Bai, K.Q.; Dan, Z.H.; Zhang, S.; Liu, Z.G. A whale optimization algorithm for global search strategy. *Small Microcomput. Syst.* **2020**, *41*, 30–35.
60. Lin, J.; He, Q.; Wang, X.; Yang, R.Y.; Ning, J.Q. Chaos-based sine cosine whale optimization algorithm. *Intell. Comput. Appl.* **2020**, *10*, 43–48+52.
61. Li, W.K. Design of dynamic encryption scheme for in-vehicle networks based on chaotic mapping. *Comput. Eng. Appl.* **2017**, *53*, 2287–2291.
62. Cui, X.W.; E, S.J.; Niu, D.X.; Wang, D.Y.; Li, M.Y. An Improved Forecasting Method and Application of China's Energy Consumption under the Carbon Peak Target. *Sustainability* **2021**, *13*, 8670. [CrossRef]